Original article

Contribution of mitochondrial dysfunction and oxidative stress to cellular premature senescence induced by antiretroviral thymidine analogues

Martine Caron[1,2], Martine Auclair[1,2], Anais Vissian[1,2], Corinne Vigouroux[1,2,3] and Jacqueline Capeau[1,2,3]*

[1]Inserm, U680, Paris, 75012 France
[2]Université Pierre et Marie Curie Paris6, UMR S680 Paris, 75012 France
[3]AP-HP, Hôpital Tenon, Service de Biochimie et Hormonologie, Paris, 75020 France

*Corresponding author: E-mail: caron@st-antoine.inserm.fr

Objectives: Treatment of HIV-infected patients is associated with early onset of aging-related comorbidities. Some of the adverse effects of antiretroviral therapy have been attributed to the mitochondrial toxicity of nucleoside reverse transcriptase inhibitors (NRTI), and it is of note that mitochondrial dysfunction and oxidative stress are involved in the aging processes. In this regard, we examined whether NRTIs could accelerate the senescence of cultured cells.

Methods: Human fibroblasts were exposed to NRTIs from culture passage 1 to 14. Cytochrome *c*-oxidase (COX) subunits 2 and 4, mitochondrial potential and mass, and reactive oxygen species (ROS) were quantified at each passage. Proliferation, cell-cycle arrest, senescence-associated β-galactosidase activity, and morphology were assessed in parallel. Mitochondrial and senescence markers were assessed in cultured murine preadipocytes and in fat samples from lipodystrophic HIV-infected patients.

Results: Stavudine and zidovudine induced mitochondrial dysfunction and increased ROS levels in fibroblasts at early culture passages, while cell division gradually slowed. At passages 8–12, fibroblasts exposed to stavudine or zidovudine but not abacavir, didanosine, lamivudine and tenofovir were senescent, on the basis of $p16^{INK4}$ and $p21^{WAF-1}$ protein expression, cell morphology and senescence-associated-β-galactosidase activity. Senescence markers and COX2 underexpression were also found in 3T3-F442A preadipocytes exposed for 7 weeks to stavudine or zidovudine, but not lamivudine, and in adipose tissue samples from lipodystrophic HIV-infected patients on antiretroviral regimens containing stavudine or zidovudine.

Conclusions: Mitochondrial changes and oxidative damage could partly explain the premature senescence of fibroblasts and adipose cells induced by stavudine and zidovudine. This suggests that thymidine analogues might be involved in the early aging-related diseases observed in some HIV-infected patients taking antiretroviral drugs.

Introduction

Some antiretroviral drugs have significant mitochondrial toxicity [1–7]. This toxicity has been linked to a wide range of severe adverse events, including lipodystrophy. Lipodystrophy becomes apparent in the medium to long term and is mainly attributed to nucleoside reverse transcriptase inhibitors (NRTI) [1,3,4,6,8–10], especially the thymidine analogues stavudine and zidovudine [8,11–13]. The mitochondrial toxicity of NRTIs has been observed in cultured cell lines [12,14,15] and in fat tissue from lipodystrophic HIV-infected patients [11,16–21]. HIV-infected patients on antiretroviral treatment are also at an increased risk of aging-related complications such as neurodegeneration, osteopenia, atherosclerosis and diabetes [22,23]. Finally, oxidant stress, probably resulting from mitochondrial dysfunction, is increased in HIV-infected patients during antiretroviral treatment [24,25].

Cellular senescence results from a signal transduction program that leads to irreversible cell growth arrest and to a distinct set of phenotypic changes [26,27]. Abundant evidence implicates mitochondria in the aging process [27–30], and experimental data show a relationship between respiratory chain dysfunction, oxidative damage and aging in most model organisms. The free-radical theory of aging postulates that intracellular reactive oxygen species (ROS) production is a major determinant

of life span. Mitochondria are the main intracellular site of oxygen reduction and, hence, the site with the greatest potential for ROS formation and sensitivity to ROS toxicity. ROS can also form in the cytosol and in peroxisomes, as by-products of specific oxidases [31].

Human skin fibroblasts offer a good model for studying the cellular aging process *in vitro* [32]. Fibroblasts proliferate readily in primary culture but have limited proliferative potential, ultimately entering a state of replicative senescence. Senescent fibroblasts show irreversible growth arrest but remain viable for long periods. They are characterized by their distinct morphology, expression of senescence-associated β-galactosidase (SA-β-galactosidase) activity [33], and upregulation of cell-cycle checkpoint inhibitors such as $p16^{INK4a}$ and $p21^{WAF-1}$ [34,35].

In this study we investigated whether a series of NRTIs could induce mitochondrial dysfunction, oxidative stress and premature senescence *in vitro*, in human skin fibroblasts and murine preadipocytes exposed to the drugs during several culture passages. We also searched for mitochondrial alteration and senescence markers in adipose tissue samples from lipodystrophic HIV-infected patients taking NRTIs.

Methods

Cell culture, fat tissue samples and treatment

Primary cultures of fibroblasts originated from subcutaneous abdominal skin of two non-obese, healthy women aged 20 and 33 years obtained during plastic surgery. They were grown in DMEM medium (Gibco® Cell Culture, InvitroGen Corporation, San Diego, CA, USA) containing 1 g/l glucose, 20 mM L-glutamine, 25 mM Hepes, 110 mg/ml sodium pyruvate, 10% fetal bovine serum (FBS, Gibco® Cell Culture), 100 U/ml penicillin and 0.1 mg/ml streptomycin (Gibco® Cell Culture) at 37°C in 5% CO_2/95% air. Murine 3T3-F442A preadipocytes were cultured in DMEM medium containing 4.5 g/l glucose, 20 mM L-glutamine, 25 mM Hepes, 10% newborn bovine serum (NBS, Gibco® Cell Culture) and antibiotics [36]. Fibroblasts (passage 1) and 3T3-F442A preadipocytes (passage 6) were treated with nucleoside reverse transcriptase inhibitors (abacavir [4 μM], didanosine [10 μM], lamivudine [10 μM], stavudine [10 μM], tenofovir [1 μM] or zidovudine [1 μM]), during the indicated passages. NRTI-treated cells were compared with control cells cultured in parallel. Didanosine, stavudine and zidovudine were obtained from Sigma Aldrich (St Quentin Fallavier, France), abacavir and lamivudine from GlaxoSmithKline (Marly-le-Roi, France) and tenofovir from Moravek Biochemicals Inc. (Brea, CA, USA). Tenofovir, but not the other NRTIs, was dissolved in dimethylsulfoxide (DMSO). DMSO at a final concentration of 0.01% did not induce cell toxicity in adipocytes [36] or fibroblasts [37].

We also used subcutaneous abdominal adipose tissue biopsy specimens from four HIV-infected lipoatrophic patients aged 41–67 years who were on NRTI-based antiretroviral regimens that included stavudine or zidovudine (but not protease inhibitors), and from four HIV-seronegative, non-diabetic, 40 to 60 year-old controls, as described elsewhere [16]. We have previously reported altered cellular morphology and mitochondrial dysfunction in fat tissue from these same HIV-infected patients [20,38]. All the patients gave their informed consent for these studies.

Western blot analysis

Cell extracts prepared as previously described [36] were subjected to SDS–PAGE, blotted onto nitrocellulose membranes and probed with antibodies against $p16^{INK4a}$ and $p21^{WAF-1}$ (ref 554070 and 556431, BD-Pharmingen, BD Biosciences, San Jose, CA, USA), the mitochondrial (mt) DNA-encoded subunit II (COX2) and the nuclear (n) DNA-encoded subunit IV (COX4) of cytochrome oxidase complex IV (ref A-6404 and A-21348, Molecular Probes, Eugene, OR, USA) and against porin (VDAC-1, ref PC548, Calbiochem, Merck Biosciences, Darmstadt, Germany). β-Actin (A-5441, Sigma Aldrich) was immunoprobed as an index of the cellular protein loading. The antibodies were detected with a chemiluminescence detection kit (GE Healthcare, Saclay, France). Gel quantification was performed with the ChemiGenius2 image analyser and software (Ozyme, St Quentin en Yvelynes, France).

Mitochondrial membrane potential and mass

We used the cationic dye JC-1 (5,5′,6,6′-tetrachloro-1,1′,3,3′-tetraethyl-benzimidazolo carbocyanine iodide, T-3168, Molecular Probes) to evaluate mitochondrial membrane potential, and the MitoTracker Red 580 probe (MTR, M-22425, Molecular Probes) to measure mitochondrial mass [14]. Cellular content was estimated by the fluorescence of DNA using Hoechst 33258. Cells were cultured in 96-well plates, washed and incubated with JC-1 (4 μg/ml), MTR (50 nM) or Hoechst 33258 (0.01 μg/ml) in DMEM without FBS for 20 min at 37°C in the dark. Quantification was performed on a plate fluorescence reader (Spectrafluor Plus, Tecan-France, Trappes, France) at 595 and 530 nm (JC-1 aggregates and monomers, respectively), 630 nm (MTR) or 460 nm (Hoechst 33258). JC-1 and MTR *in situ* labelling was also examined by fluorescence microscopy.

ROS production

We used the CM-H_2DCFDA derivatives (5- and 6-chloromethyl-2′,7′-dichlorodihydrofluorescein

diacetate, acetyl ester, C6827, Molecular Probes) as cell-permeant indicators of ROS. Cells were cultured in 96-well plates, washed and incubated with CM-H_2DCFDA (9 μM) in DMEM without FBS for 20 min at 37°C in the dark. Fluorescence was quantified on a plate reader at 520 and 460 nm, respectively. Oxidized CM-H_2DCFDA *in situ* localization was also examined by fluorescence microscopy.

ROS production was also detected by measuring the reduction of nitroblue tetrazolium (NBT, Sigma-Aldrich). Cells were incubated in medium containing 0.2% NBT for 90 min. Dark blue reduced NBT, dissolved in DMSO, was assessed at 560 nm in a spectrophotometer.

Population doubling level

The population doubling level (PDL) was calculated as previously described [39] as $\log_2 (D/D_0)$, where D_0 and D are the numbers of cells at seeding and harvesting, respectively. Senescence was considered complete when cells were unable to complete one PDL during a 4-week period, including three consecutive weeks of refeeding with fresh complete medium. Control fibroblasts and 3T3-F442A preadipocytes did not reach replicative senescence at passages 18 and 15, respectively. The cumulative population doubling level (CPDL) was determined by adding the PDL values measured at each culture passage.

Cellular BrdU labelling

Dividing cells were identified by measuring bromodeoxyuridine (BrdU) incorporation according to the manufacturer's instructions (BrdU *in situ* detection kit, BD Biosciences Pharmingen, San Diego, CA, USA). Briefly, half-confluent cells were incubated for 16 h with BrdU (15 μM), then fixed and permeabilized. Anti-BrdU antibodies, streptavidine-horse radish peroxidase and the diaminobenzidine (DAB) substrate were then added successively for 60, 30 and 5 min. Dividing cells (red-brown), examined by phase contrast microscopy at 20× magnification, were counted in four randomly selected fields and expressed as a percentage of total cells.

Senescence-associated β-galactosidase assay

β-Galactosidase activity at pH 6 has been widely used as a biomarker of cellular senescence *in vivo* and *in vitro* [33]. Cells on cover slips were fixed for 3–5 min at 22°C with 2% formaldehyde/0.2% glutaraldehyde and incubated overnight at 37°C in 1 mg/ml 5-bromo-4-chloro-3-indolyl-β-D-galactoside (X-gal), 40 mM citric acid-sodium phosphate (pH 6 or 4), 5 mM potassium ferricyanide, 5 mM potassium ferrocyanide, 150 mM NaCl and 2 mM $MgCl_2$. The blue X-gal-stained cells observed at pH 6 and pH 4 were examined by phase contrast microscopy (20× magnification) and counted in eight fields (500 cells). The ratio of pH 6- to pH 4-positive blue cells, which specifically represents SA-β-galactosidase activity, was calculated.

Statistical analysis

All experiments were performed at least in triplicate. All quantitative results were expressed as mean ±SEM. Statistical significance was determined with the parametric Student's *t*-test. *P*-values <0.05 were considered significant.

Results

Some NRTIs induce mitochondrial dysfunction in cultured fibroblasts

Stavudine and zidovudine, two NRTIs previously shown to induce mitochondrial toxicity in adipocytes [6,11,14,15], also altered mitochondrial function in cultured fibroblasts (Figure 1). They reduced the mitochondrial membrane potential, as shown by the JC-1 aggregate/monomer ratio, which was decreased by 35–50% at early (3–4) and late (9–13) passages (Figure 1A, left), as compared with untreated cells. Abacavir, didanosine, lamivudine and tenofovir did not induce mitochondrial depolarization at passages 7–8 (Figure 1A, right), and all along the culture passages up to passage 13 (not shown). Further indication of the specificity of the JC-1 assay was supported by fluorescence microscopy. Indeed, in untreated fibroblasts, JC-1 red-orange fluorescence is mainly localized in the cytoplasm in rod-like structures that are typical of mitochondria (data not shown).

Stavudine and zidovudine, but not other NRTIs, markedly reduced the protein expression of COX2, a mtDNA-encoded subunit of cytochrome oxidase complex IV of the respiratory chain, and increased expression of the nDNA-encoded COX4 subunit of the same complex. The expression of the nDNA-encoded mitochondrial VDAC-1 (porin) was also increased (Figure 1B, left). Densitometric quantification indicated that stavudine and zidovudine reduced the ratio COX2/COX4 by 3.1-fold and 4.9-fold, respectively (Figure 1B, right), and increased the ratio COX4/β-actin or porin/β-actin by 1.5- to 2-fold. The other NRTIs tested had no significant effect on the protein expression of COX2, COX4 or porin.

MTR dye fluorescence indicated that stavudine and zidovudine significantly increased the mitochondrial mass per cell (by three- to fourfold) in fibroblasts (Figure 1C, left). The effect was maximal at passage 5–6 and did not vary thereafter, arguing for a rapid increase in mitochondrial biogenesis. Abacavir, didanosine, lamivudine and tenofovir did not modify the mitochondrial mass as compared with untreated fibroblasts. The increased mitochondrial proliferation in response to

Figure 1. NRTIs induce mitochondrial dysfunction in human fibroblasts

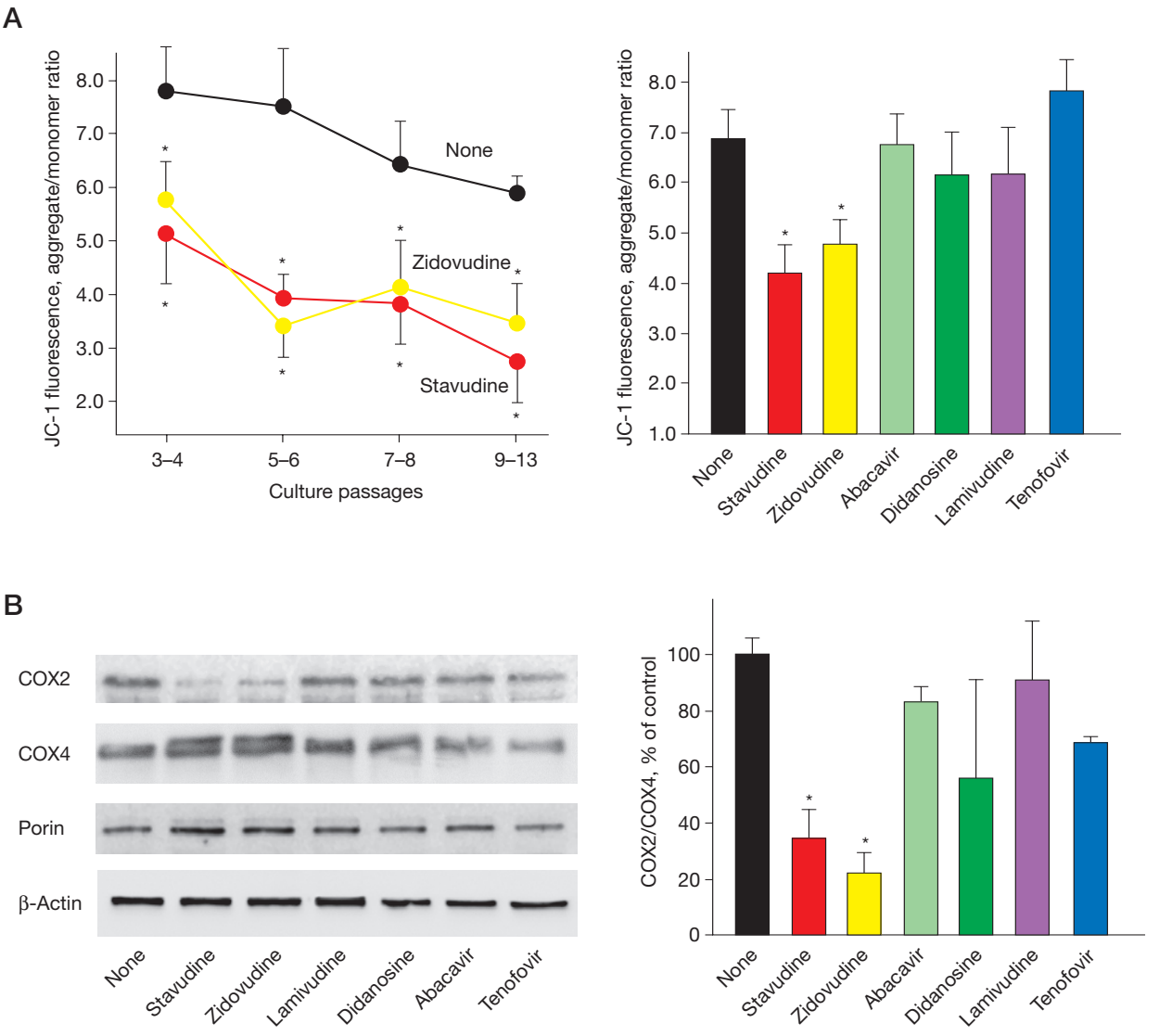

Fibroblasts were cultured from passages 1 to 13 in 96-well plates in the presence or absence of the indicated nucleoside reverse transcriptase inhibitor (NRTI; see colour code). **(A)** Cells were incubated for 30 min with JC-1 at 37°C in the dark. Monomer green fluorescence was quantified on a fluorescence plate reader at 530 nm and aggregate red–orange fluorescence at 595 nm. The results are expressed as the ratio aggregate/monomer fluorescence at the indicated passages (left), and at passages 7–8 (right). Values are means ±SEM of three experiments performed in quadruplicate. **(B)** Western blots of fibroblast lysates (left) were revealed with antibodies against the mitochondrial proteins cytochrome c oxidase IV subunits 2 and 4 (COX2, COX4) and porin and against β-actin, as indicated. Representative blots (passages 5–6) from triplicate experiments are shown. The COX2/COX4 protein expression ratio was determined by densitometric scanning and expressed as a percentage of control (mean ±SEM) (right). **(C)** Mitochondrial mass was measured by MitoTracker Red (MTR) labelling at 630 nm and normalized to the cellular DNA content determined in parallel by Hoechst 33258 staining at 460 nm. MTR/DNA fluorescence was assessed at all passages (3–12; colour code as in A and B). The results are the means ±SEM at the indicated passages. Experiments were performed at least four times on quadruplicate samples (left). Living cells (passage 8) were stained *in situ* using MTR (red labelling) and examined by fluorescence microscopy. Scale bar represents 20 µm (right). *P<0.05 as compared with control cells.

medium- or long-term incubation with stavudine or zidovudine was confirmed by *in situ* fluorescence microscopy, assessed at passage 8 (Figure 1C, right).

Stavudine and zidovudine increase ROS production

ROS production was evaluated indirectly by measuring the oxidation status of the permeant derivatives CM-H_2DCFDA and the reduction of NBT. In fibroblasts exposed to stavudine or zidovudine (Figure 2A) CM-H_2DCFDA oxidation increased in two stages, with a 2.5- to threefold rise at passages 3 to 6 followed by a further increase at passages 7–9 (five- to eightfold higher than the control value). Incubation of cells with abacavir, lamivudine, didanosine or tenofovir did not increase ROS production at any passage (Figure 2A, top). Fluorescence microscopy (passage 8, Figure 2A, bottom)

Figure 1. Continued

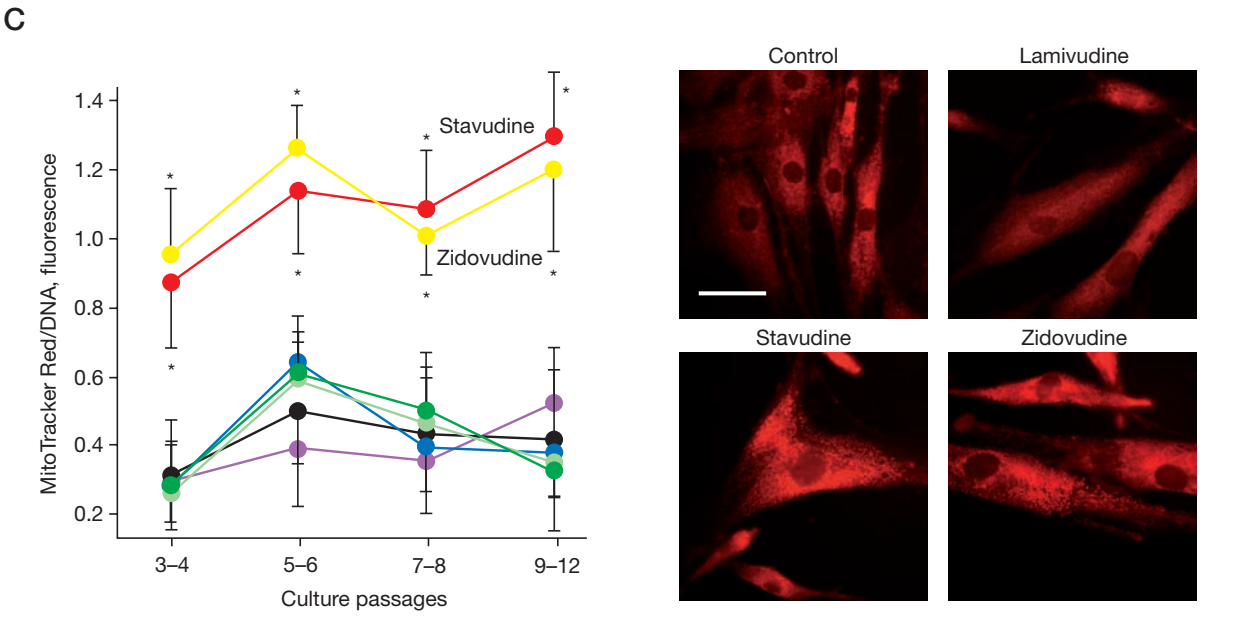

confirmed the increased level of ROS in cells exposed to stavudine or zidovudine, as compared with controls. The green fluorescence of CM-H_2DCFDA was predominantly located near the nucleus. Irrelevant green fluorescence was observed in untreated cells and in cells exposed to abacavir, didanosine, lamivudine or tenofovir (Figure 2A and data not shown).

The gradual increase in ROS production induced by stavudine and zidovudine was also observed by measuring NBT reduction, which was significantly increased at all studied passages (3–13) as compared with control cells and cells incubated with abacavir, lamivudine, didanosine or tenofovir (Figure 2B). At passages 7–8, didanosine significantly increased NBT reduction as compared with control cells. However, didanosine had no effect on NBT reduction at higher culture passages (9–13) and failed to increase significantly CM-H_2DCFDA oxidation at any culture passage (Figure 2A, top).

Fibroblasts incubated with stavudine or zidovudine show reduced proliferative and replicative capacity

We searched for premature senescence in NRTI-incubated cells. The PDL of untreated fibroblasts remained stable up to passage 15, at 2.06 ±0.034 (Figure 3A). In contrast, the proliferation rate of fibroblasts incubated with stavudine or zidovudine fell gradually with successive passages. Half-maximal inhibition of PDL and arrest of cell division (PDL<0.5) were observed at passages 8–9 and 12–13, respectively, and were similar in fibroblasts incubated with stavudine or zidovudine. Up to passage 15, abacavir, didanosine, lamivudine and tenofovir had no significant effect on the rate of proliferation.

In keeping with these results, the cumulative PDL (CPDL) calculated from passages 2 to 15 was significantly and similarly reduced in cells exposed to stavudine and zidovudine, as compared with untreated cells (7.69 ±0.78 and 7.71 ±0.77, respectively, versus 14.45 ±0.27). The CPDL of cells incubated with the other NRTIs was not significantly different from the control value (not shown).

Fibroblasts incubated with stavudine or zidovudine also exhibited a striking decrease in their replicative capacity measured in terms of BrdU incorporation in half-confluent cells (60–80% reduction at passages 6–8), as compared with control cultures and in cultures exposed to abacavir, didanosine, lamivudine or tenofovir (Figure 3B, top). Interestingly, most fibroblasts incubated with stavudine and zidovudine were enlarged and flattened (Figure 3B, bottom) – morphological changes typically associated with senescence [26].

Arrest of cell division was also indicated by the increased protein expression of $p16^{INK4}$ and $p21^{WAF-1}$, two cell-cycle checkpoint inhibitors that participate in the setup of the senescence program [34,35]. $P16^{INK4}$ and $p21^{WAF-1}$ were overexpressed by 250–400% in cells exposed to stavudine or zidovudine at passages 6–8 (Figure 4A). At the same passages, $p16^{INK4}$ and $p21^{WAF-1}$ protein expression was not different between control cells and cells exposed to the other NRTIs studied (Figure 4A and not shown).

Fibroblasts incubated with stavudine and zidovudine prematurely acquire a senescent phenotype

Strong cellular staining for X-gal at pH 4, indicating physiological lysosomal β-galactosidase activity, was detected in control and NRTI-treated fibroblasts. SA-β-galactosidase activity, assessed at pH 6, was absent in control cells up to passage 14, but present in cells incubated with stavudine or zidovudine (Figure 4B and data not shown). The number of X-gal-stained cells at pH 6 increased 40- to 60-fold, accounting for 35–85% of all cells. Little or no SA-β-galactosidase activity was detected in fibroblasts incubated with abacavir, didanosine, lamivudine and tenofovir up to passage 12 (Figure 4B and not shown). Microscopic examination (Figure 4B, bottom) showed that X-gal-stained fibroblasts at pH 6 incubated with stavudine or zidovudine displayed senescence-associated morphological changes.

Figure 2. NRTIs increase ROS production in human fibroblasts

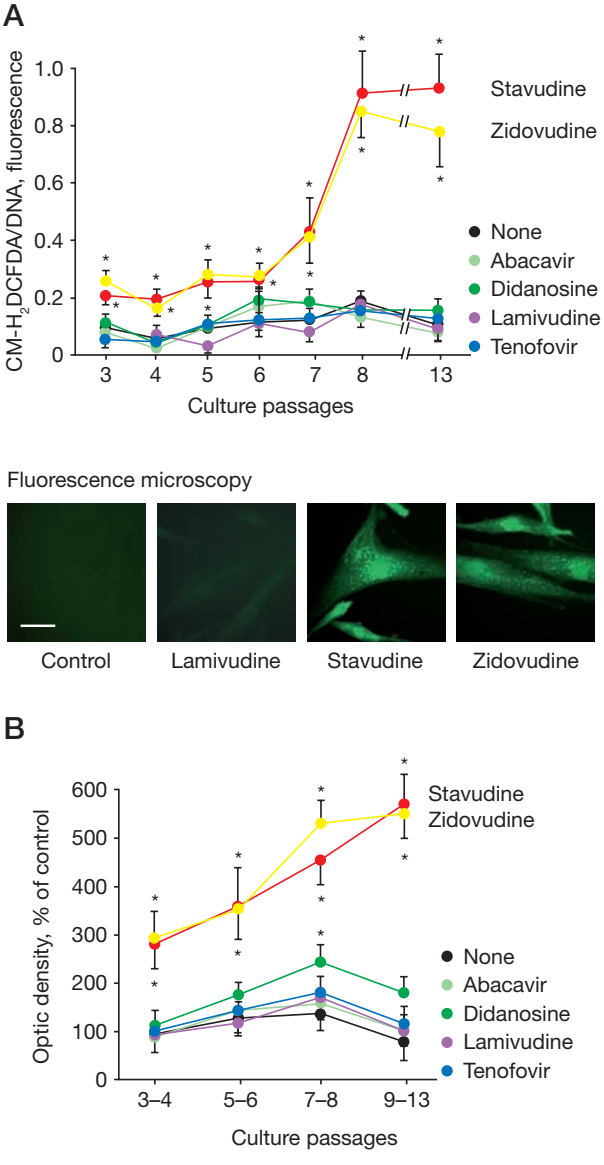

(A) ROS production was assessed at the indicated passages by the fluorescence of the oxidized forms of CM-H_2DCFDA derivatives (at 520 nm) and was normalized to the DNA content. Results are the mean ±SEM (top). CM-H_2DCFDA green fluorescence was examined *in situ* in living cells at passage 8 by fluorescence microscopy. Scale bar represents 20 µm (bottom). **(B)** ROS production was also measured in terms of the reduction of nitroblue tetrazolium (NBT). Results are expressed as a percentage of control (mean ±SEM) of three independent experiments performed in triplicate. **P*<0.05 as compared with control cells.

Expression of senescence markers in adipose cells and HIV patients' fat tissue

Mitochondrial function and oxidative stress in 3T3-F442A murine preadipocytes incubated with stavudine or zidovudine for 6 weeks (from passages 7–13; Figure 5A) were also evaluated. In preadipocytes exposed to stavudine, JC-1 aggregation and MTR fluorescence fell and rose, respectively, as a function of the duration of treatment, consistent with a reduction of the mitochondrial membrane potential and an increased mitochondrial mass. Oxidative stress was also observed in preadipocytes incubated for 1 week and more strikingly for 6 weeks with stavudine, as shown by two- and eightfold increase in CM-H_2DCFDA oxidation (Figure 5A). A 6-week incubation with stavudine or zidovudine, but not with lamivudine, also increased NBT reduction (by twofold) in murine preadipocytes (Figure 5A).

Continuous exposure of 3T3-F442A preadipocytes to stavudine or zidovudine, but not lamivudine, was associated with a gradual decline in the PDL value (fourfold decrease at week 6 of treatment; Figure 5B, left). In keeping with the arrest of cell division, preadipocytes incubated with stavudine and zidovudine expressed increased levels of $p16^{INK4}$ and $p21^{WAF1}$ (Figure 5B, right). Accelerated senescence was also indicated by the increased pH 6/4 β-galactosidase activity ratio (0.073 ±0.009 and 0.597 ±0.198 in control and stavudine-treated cells, respectively, at weeks 5–6 of treatment; P=0.0287) and by the enlarged and flattened morphology of cells exposed to stavudine or zidovudine (not shown).

Subcutaneous adipose tissue samples from lipodystrophic HIV-infected patients on NRTI-based therapy containing stavudine or zidovudine without protease inhibitors had a markedly reduced COX2/COX4 expression ratio and increased levels of $p16^{INK4}$ and $p21^{WAF-1}$, as compared with fat samples from healthy HIV-seronegative subjects (Figure 5C, left). Protein expression of COX4 and porin, adjusted to the β-actin level, was increased in fat samples from HIV-infected patients as compared with control (Figure 5C, right), suggesting that mitochondrial biogenesis could be enhanced in adipose tissue from NRTI-treated patients. These data indicate that adipose tissue in lipodystrophic HIV-infected patients treated with stavudine or zidovudine exhibited signs of mitochondrial dysfunction and senescence.

Discussion

HIV-infected patients tend to develop age-related complications such as diabetes, atherosclerosis, neurodegenerative disorders, osteopenia, sarcopenia and general loss of lean body mass earlier than the general population [40–43]. Moreover, the rate at which lipodystrophy worsens in HIV-infected patients increases with age [44,45], and middle-aged HIV-infected patients have an immune status [46] and frailty-related phenotype similar to that of older healthy subjects [47].

The toxicity of HIV antiretroviral treatments has been largely attributed to the mitochondrial toxicity of NRTIs [1,3–5,7,9,11]. Severe adverse events have been related to mitochondrial dysfunction, including lactic acidosis, hepatic steatosis, neuropathy, cardiomyopathy, pancreatitis [3–5,7] and lipoatrophy [6,10]. Mitochondrial toxicity in this setting has been more specifically attributed to the thymidine analogues stavudine and zidovudine. Several groups, including ours, have demonstrated that these two thymidine analogues induce mitochondrial alterations not only in cultured cells [12,14,15] but also *in vivo*, in the cells and fat tissue of HIV-infected patients [6,11,13,17,18,20]. A further argument for the mitochondrial toxicity of NRTI is provided by the study of Mallon *et al*. [48] reporting that a 2-week treatment of healthy individuals with stavudine or zidovudine (in association with lamivudine) promoted adipose tissue mitochondrial dysfunctions.

Mitochondria dysfunction and mitochondrial oxidative stress are known key factors in several aging theories [29,30]. The free-radical theory of aging holds that aging and associated degenerative disorders can be attributed to deleterious effects of ROS. ROS are by-products of cellular metabolic pathways and function as crucial second messengers in a variety of intracellular signalling pathways [30]. They are primarily generated by the mitochondrial electron transport chain. Excessive intracellular generation of ROS on the one hand, and deficient anti-oxidant defence systems on the other, lead to a state of 'oxidative stress'. Direct or indirect ROS involvement has been documented in numerous diseases and the mitochondrial network was identified as a prime target of oxidative damage [29,30].

In the present study we report that the thymidine analogues stavudine and zidovudine, but not the NRTIs abacavir, didanosine, lamivudine and tenofovir, induced mitochondrial dysfunction, increased mitochondrial proliferation and enhanced ROS production in cultured human fibroblasts. Moreover, 3T3-F442A preadipocytes incubated with stavudine or zidovudine for 6 weeks harboured markers of mitochondrial dysfunction, as did fat biopsy specimens from lipodystrophic HIV-infected patients on antiretroviral regimens containing these thymidine analogues. In cultured fibroblasts and preadipocytes, mitochondrial disorders and oxidative stress occurred early, beginning after only 1 week of treatment with stavudine or zidovudine, were maximal at week 3, and persisted throughout subsequent culture passages. This is in accordance with the rapid

Figure 3. NRTIs reduce proliferative and replicative capacity of human fibroblasts

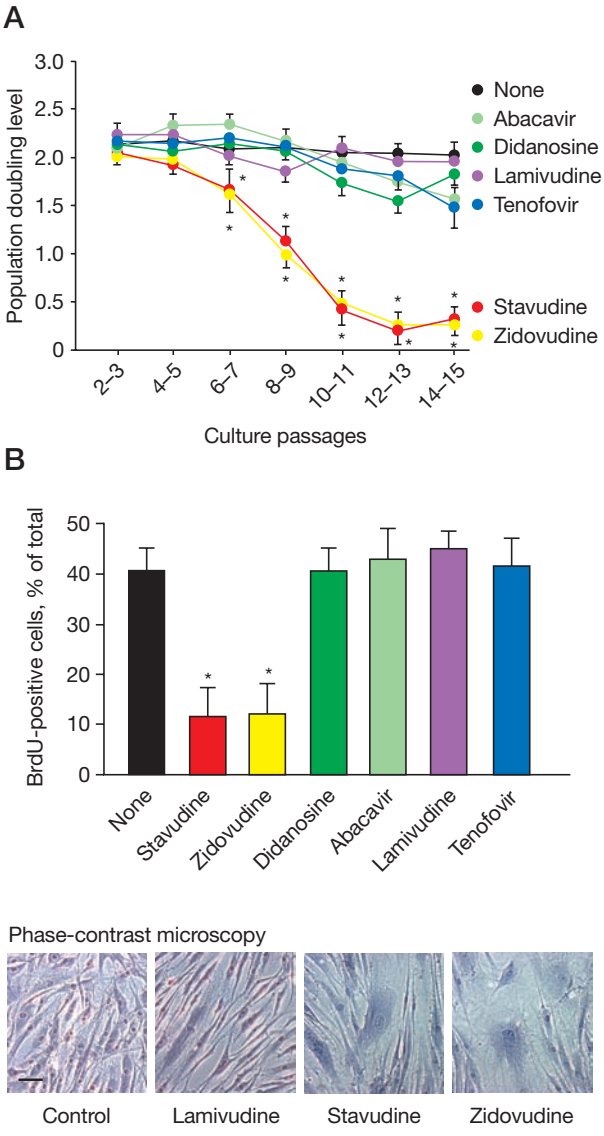

(A) The population doubling level (PDL) was calculated as $\log_2 (D/D_0)$. Mean PDL values ±SEM at the indicated passages are shown. **(B)** BrdU staining was performed on half-confluent fibroblasts as indicated in the *Methods*, and visualized by conventional phase-contrast microscopy. The percentage of the mean ±SEM of dividing cells at passage 6–8 was assessed by counting total and BrdU-stained cells (top). Scale bar represents 40 µm. Note the altered cell number and morphology of fibroblasts incubated with stavudine and zidovudine (passage 9; bottom).*P<0.05 as compared with control cells.

deterioration of mitochondrial functions in adipose tissue from healthy subjects treated for 2 weeks with stavudine or zidovudine [48]. In our study, mitochondrial dysfunction was evidenced by three means: altered mitochondrial membrane potential, decreased expression of mtDNA-encoded mitochondrial proteins, and increased mitochondrial proliferation. NRTI-induced mitochondrial proliferation, observed by enhanced MTR staining and increased expression of two nDNA-encoded mitochondrial proteins (COX4 and porin), has also been reported in cultured adipocytes [15] and in patients' fat samples [21,38]. Mitochondrial biogenesis

Figure 4. NRTIs induce cell-cycle arrest and premature senescence in human fibroblasts

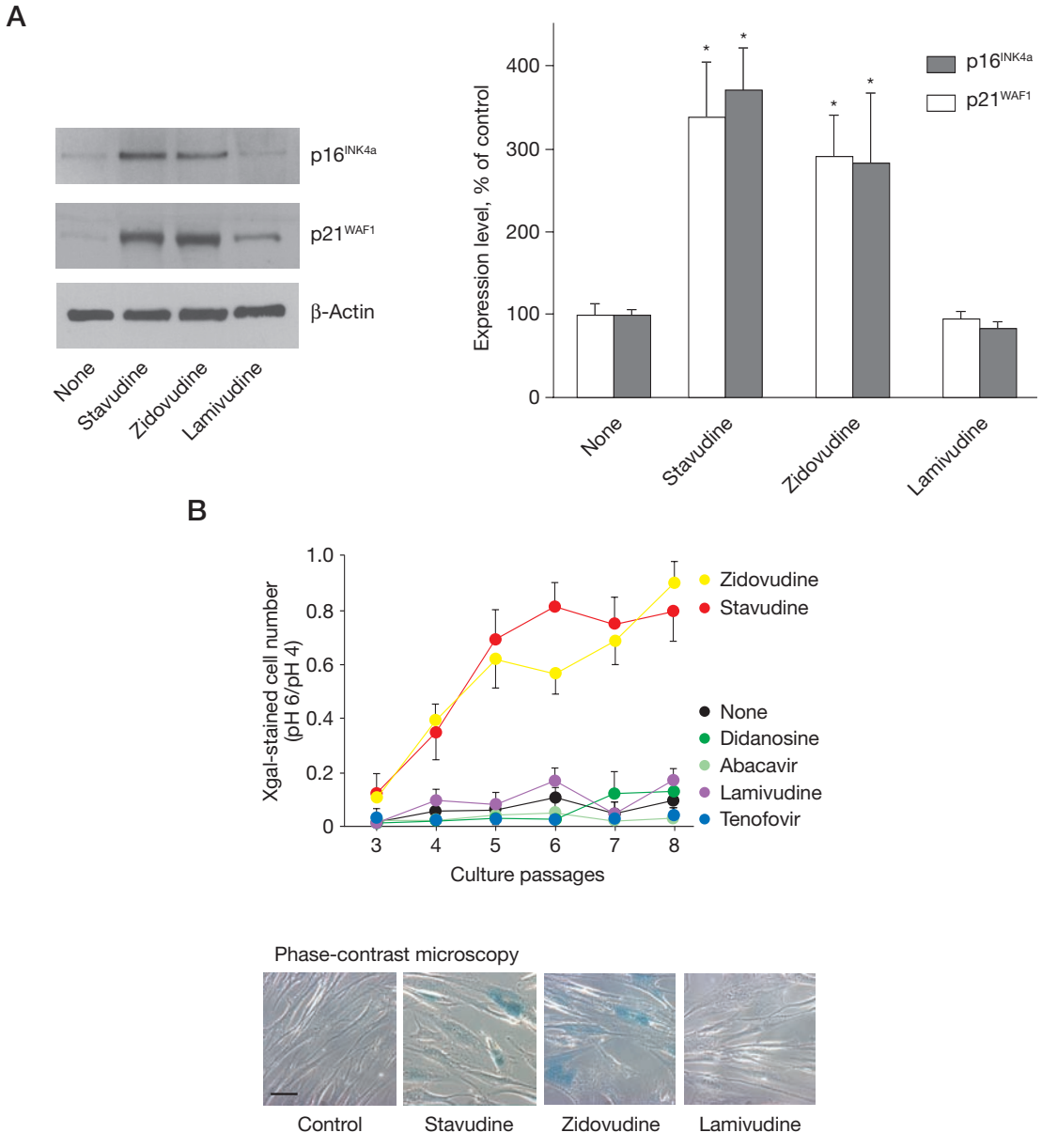

(A) Western blots of fibroblast lysates (passage 10) were revealed with antibodies against $p16^{INK4}$, $p21^{WAF-1}$ and β-actin, as indicated. Experiments were performed in triplicate. Representative blots are shown (left). The protein expression ratio of $p16^{INK4}$ or $p21^{WAF-1}$/β-actin was determined by densitometric scanning and expressed as a percentage of control (mean ±SEM; right). **(B)** Physiological lysosomal (pH 4) and senescence-associated-β-galactosidase (pH 6) activities were assessed by cellular X-gal blue staining. The ratio of pH 6/pH 4 positive blue cells was calculated after microscopic examination of 500 cells at the indicated passages (3–8) (top). Experiments were performed in triplicate. Representative conventional micrographs of X-gal-stained cells (passage 7) at pH 6 are shown (bottom). Scale bar represents 40 µm. Note the senescence-associated flattened and enlarged morphology of X-gal-stained cells incubated with stavudine and zidovudine.*P<0.05 as compared with control cells.

might be considered as a compensatory mechanism contributing to the relative preservation of mitochondrial functions. However, it can have deleterious consequences in genetic mitochondriopathies [49] suggesting, as in the present study, that newly formed mitochondria could be non-functional. Decreased mtDNA levels resulting from inhibition of DNA polymerase γ, is considered as a major marker of mitochondrial defects related to antiretroviral treatments [1,7,13]. However, dissociation between the mtDNA content and the expression of mtDNA-encoded mitochondrial proteins under NRTI exposure has been reported [19,48]. In the

Figure 5. Mitochondrial dysfunction and senescence markers in 3T3-F442A preadipocytes exposed to NRTIs **(A,B)** and in adipose tissue from HIV-seronegative controls and lipodystrophic HIV-infected patients under NRTI therapy **(C)**

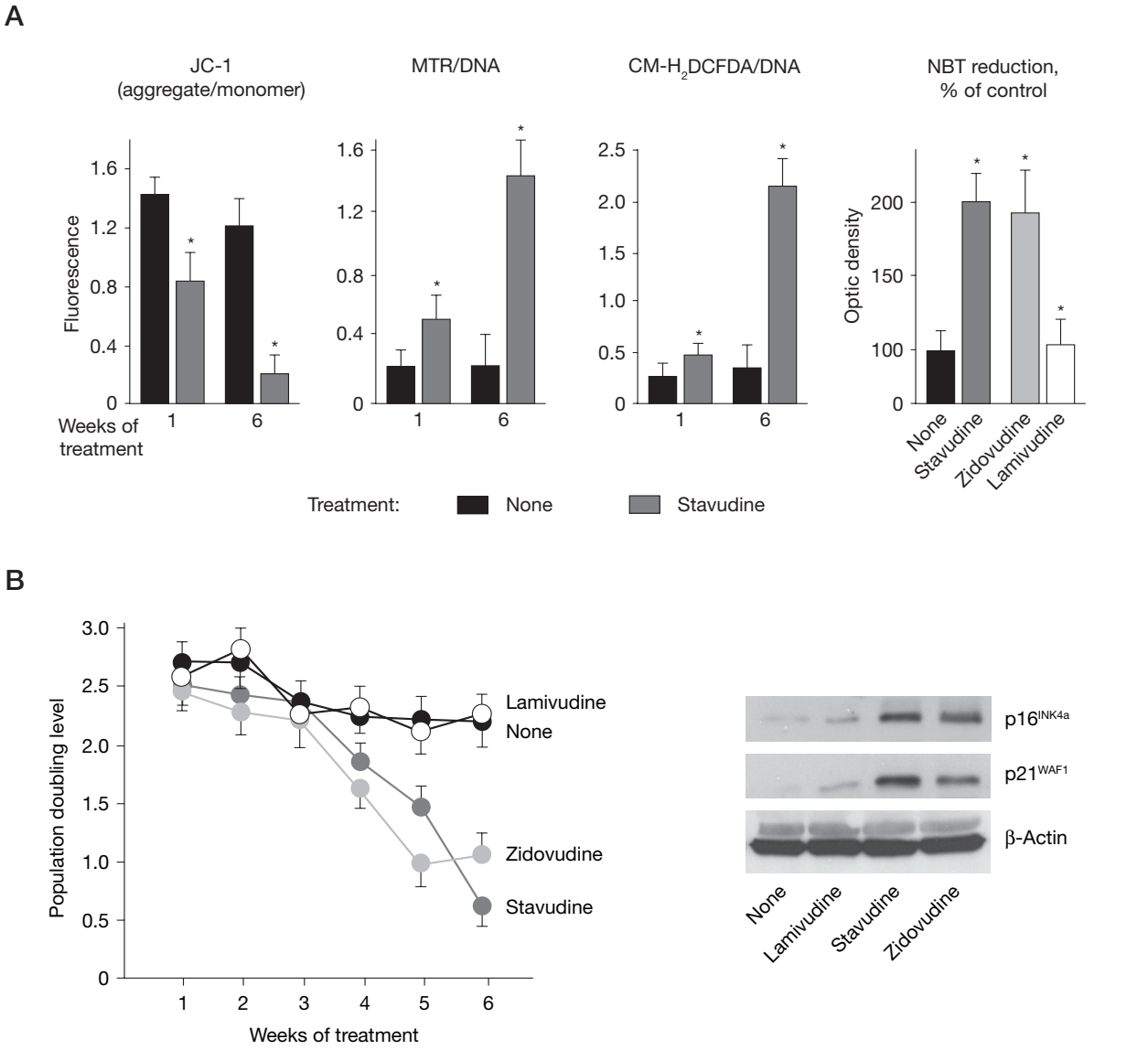

(A) Mitochondrial dysfunction and ROS production were assessed at the indicated weeks of NRTI incubation, by JC-1 aggregation and MitoTracker Red (MTR) labelling and by the oxidation of CM-H_2DCFDA derivatives and reduction of nitroblue tetrazolium (NBT; see the *Methods* and legends of Figures 1 and 2). NBT reduction was assessed after 6 weeks of NRTI incubation. The experiments were performed in triplicate. **(B)** Preadipocytes were treated with the indicated NRTI. Mean PDL values ±SEM at the indicated passages are shown (left). Western blots of cell lysates were revealed with antibodies against $p16^{INK4}$, $p21^{WAF1}$ and β-actin as indicated. Representative blots of preadipocytes exposed to NRTI (for 6 weeks) performed in triplicate are shown (right). **(C)** Lysates of subcutaneous fat tissue from control HIV-seronegative subjects or lipodystrophic HIV-infected patients under stavudine or zidovudine therapy were submitted to western blot with the indicated antibodies. Representative blots (performed in triplicate) are shown (left). COX2/COX4, COX4/β-actin and porin/β-actin protein ratios were determined by scanning densitometry and expressed as a percentage of control (mean ±SEM) (right).*P<0.05 as compared with control cells.

Figure 5. Continued

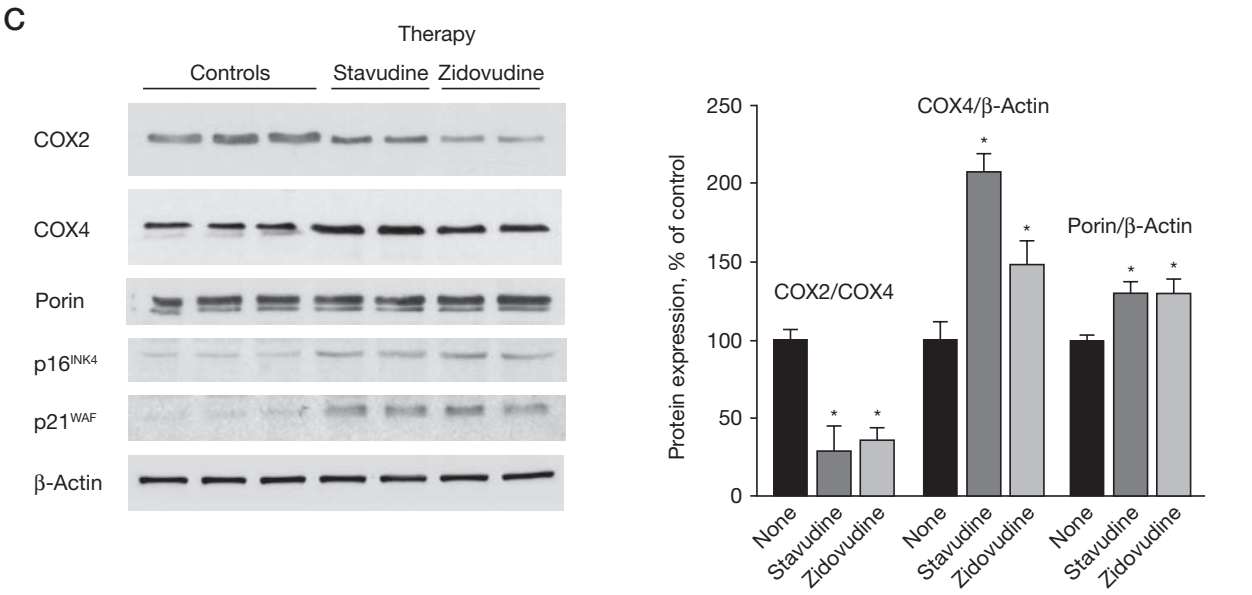

present study inconclusive preliminary data have been obtained on the effect of a 4-week incubation of fibroblasts with stavudine, zidovudine or lamivudine on mtDNA level, whereas during the same period the thymidine analogues markedly altered mitochondrial membrane potential, COX2, COX4 and porin protein expression, mitochondrial mass and ROS production, consistent with their mitochondrial toxicity. It is possible that the mtDNA level would decrease at later culture passages in fibroblasts, a time at which ROS level and toxicity were markedly enhanced. We previously reported [15] that 3T3-F442A adipocytes incubated for 4 weeks with stavudine or zidovudine had a severe decrease in mtDNA, as compared with untreated adipocytes, suggesting that the severity of mtDNA alterations could be tissue-specific.

We show here that mitochondrial toxicity of stavudine and zidovudine is associated with a rapid and sustained increase of ROS production in human fibroblasts and murine preadipocytes. Interestingly, short-term incubation of human adipocytes or macrophages with these NRTIs also induced an oxidative stress [50]. Increased oxidative stress and abnormal antioxidant defenses have also been demonstrated in HIV-infected patients, including patients treated with NRTIs [24,25,51].

Stavudine and zidovudine triggered the senescence program prematurely in cultured human skin fibroblasts and 3T3-F442A preadipocytes. Indeed, the cells continuously exposed to stavudine or zidovudine showed a gradual slowing of cell proliferation and division, acquired the morphology of senescent cells, and expressed SA-β-galactosidase activity. At later passages they expressed the cell-cycle checkpoint inhibitors $p16^{INK4a}$ and $p21^{WAF-1}$, a finding consistent with cell cycle arrest. In contrast, long-term incubation with abacavir, lamivudine and tenofovir did not alter mitochondrial function or the ROS level and did not trigger premature senescence, in accordance with their weak mitochondrial toxicity [52,53]. It is noteworthy in this respect that these NRTIs carry a lower risk of lipodystrophy than stavudine or zidovudine [10].

Interestingly, the effects of the thymidine analogues on mitochondrial markers and oxidative stress in human fibroblasts were maximal after 3 weeks of treatment, whereas senescence markers were maximally altered after 13 weeks. A similar lag time between mitochondrial toxicity and senescence entry was also observed in 3T3-F442A preadipocytes treated with stavudine. This sequence of events points to a role of mitochondrial oxidative stress in NRTI-induced premature senescence, although we could not produce definitive experimental evidence for a direct relationship. Experiments using antioxidants might help to elucidate the role of ROS in NRTI-induced premature senescence. We could not exclude that cytosolic ROS originating from the NADPH oxidase pathway could contribute to senescence triggering and, in a vicious circle, further increase mitochondrial alterations.

Although an association between NRTI-induced mitochondrial alterations, ROS hyperproduction and senescence has been shown *in vitro*, in proliferating cells (fibroblasts and preadipocytes), it is not possible to extrapolate to other tissues and especially

non-proliferative cells. In the present setting, the effect of the drugs could relate not only to the increased number of replicative rounds, but also to the length of the exposure. It would be interesting to assess whether older fibroblasts, exposed to the drugs at later passages, would be more sensitive to the deleterious action of stavudine or zidovudine. It also remains to be investigated whether the setup of the senescence program triggered by the thymidine analogues could be blocked or reversed by arresting or substituting the drugs.

The pathophysiological relevance of these findings is supported by the detection of markers of mitochondrial dysfunction and senescence in fat tissue from lipodystrophic HIV-infected patients on stavudine- or zidovudine-based antiretroviral regimens, although data on the mitochondria and senescence status of untreated HIV-infected patients are lacking. Otherwise, the mechanisms whereby HIV-infected patients develop several age-related comorbidities are obviously multifactorial, resulting from therapy with aggressive NRTIs, but also from HIV infection or co-treatment with other antiretrovirals. Accordingly, we recently reported that some protease inhibitors can trigger premature senescence via a mitochondrial oxidative stress, *in vitro*, in cultured fibroblasts, and *in vivo* at the fat tissue level of HIV-infected patients [37]. Protease inhibitor effects were shown to result from the cellular stress linked to farnesylated prelamin A, a nuclear precursor of lamin A, the accumulation of which leads to severe genetically determined premature ageing syndromes [54]. Although prelamin A accumulation was not observed in NRTI-treated cells (data not shown), protease inhibitors and NRTIs may work in synergy to trigger a mitochondrial oxidative stress and aggravate age-related diseases in HIV-infected patients.

Interestingly, premature aging syndromes are known to be associated with lipodystrophy [54] and the prevalence and severity of the lipodystrophy phenotype in HIV-infected patients under antiretrovirals both increased with age [44,45]. This suggests that premature adipose tissue aging could be one mechanism whereby antiretrovirals induce lipodystrophy.

Taken together these results show the contribution of mitochondrial dysfunction and oxidative stress to cellular premature senescence induced by antiretroviral thymidine analogues. Validation of these results with longitudinal cohorts of HIV-infected patients is required to confirm the link between the toxicity of antiretroviral treatment and aging-related comorbidities.

Acknowledgements

We thank P Levan for providing the adipose tissue samples and V Jan for preparing the fat samples extracts. This work was supported by grants from INSERM, Agence Nationale pour la Recherche sur le SIDA, Sidaction and from European Union's FP6 Life Science, Genomics and Biotechnology for Health (LSHM-CT-2005-018690).

Disclosure statement

MC received a travel grant and honoraria for conference attendance from Glaxo Smith Kline. CV received a travel grant from Gilead and honoraria for conference attendance from Bristol Myers Squibb. JC received travel grants and/or honoraria for conferences from Glaxo Smith Kline, Bristol Myers Squibb, Vertex, Abbott, Roche and Sanofi-Aventis.

References

1. Brinkman K, Smeitink JA, Romijn JA, Reiss P. Mitochondrial toxicity induced by nucleoside-analogue reverse-transcriptase inhibitors is a key factor in the pathogenesis of antiretroviral-therapy-related lipodystrophy. *Lancet* 1999; **354**:1112–1115.
2. Carr A, Cooper DA. Adverse effects of antiretroviral therapy. *Lancet* 2000; **356**:1423–1430.
3. Lewis W, Day BJ, Copeland WC. Mitochondrial toxicity of NRTI antiviral drugs: an integrated cellular perspective. *Nat Rev Drug Discov* 2003; **2**:812–822.
4. Cossarizza A, Moyle G. Antiretroviral nucleoside and nucleotide analogues and mitochondria. *AIDS* 2004; **18**:137–151.
5. Gerschenson M, Brinkman K. Mitochondrial dysfunction in AIDS and its treatment. *Mitochondrion* 2004; **4**:763–777.
6. Villarroya F, Domingo P, Giralt M. Lipodystrophy associated with highly active anti-retroviral therapy for HIV infection: the adipocyte as a target of anti-retroviral-induced mitochondrial toxicity. *Trends Pharmacol Sci* 2005; **26**:88–93.
7. Pinti M, Salomoni P, Cossarizza A. Anti-HIV drugs and the mitochondria. *Biochim Biophys Acta* 2006; **1757**:700–707.
8. Barile M, Valenti D, Quagliariello E, Passarella S. Mitochondria as cell targets of AZT (zidovudine). *Gen Pharmacol* 1998; **31**:531–538.
9. Dalakas MC, Semino-Mora C, Leon-Monzon M. Mitochondrial alterations with mitochondrial DNA depletion in the nerves of AIDS patients with peripheral neuropathy induced by 2'3'-dideoxycytidine (ddC). *Lab Invest* 2001; **81**:1537–1544.
10. Nolan D, Mallal S. The role of nucleoside reverse transcriptase inhibitors in the fat redistribution syndrome. *J HIV Ther* 2004; **9**:34–40.
11. Hammond E, Nolan D, James I, Metcalf C, Mallal S. Reduction of mitochondrial DNA content and respiratory chain activity occurs in adipocytes within 6–12 months of commencing nucleoside reverse transcriptase inhibitor therapy. *AIDS* 2004; **18**:815–817.
12. Velsor LW, Kovacevic M, Goldstein M, *et al*. Mitochondrial oxidative stress in human hepatoma cells exposed to stavudine. *Toxicol Appl Pharmacol* 2004; **199**:10–19.
13. Walker UA, Bauerle J, Laguno M, *et al*. Depletion of mitochondrial DNA in liver under antiretroviral therapy with didanosine, stavudine, or zalcitabine. *Hepatology* 2004; **39**:311–317.
14. Caron M, Auclair M, Lagathu C, *et al*. The HIV-1 nucleoside reverse transcriptase inhibitors stavudine and zidovudine alter adipocyte functions *in vitro*. *AIDS* 2004; **18**:2127–2136.

15. Walker UA, Auclair M, Lebrecht D, *et al*. Uridine abrogates the adverse effects of antiretroviral pyrimidine analogues on adipose cell functions. *Antivir Ther* 2006; **11**:25–34.
16. Bastard JP, Caron M, Vidal H, *et al*. Association between altered expression of adipogenic factor SREBP1 in lipoatrophic adipose tissue from HIV-1-infected patients and abnormal adipocyte differentiation and insulin resistance. *Lancet* 2002; **359**:1026–1031.
17. Boyd MA, Carr A, Ruxrungtham K, *et al*. Changes in body composition and mitochondrial nucleic acid content in patients switched from failed nucleoside analogue therapy to ritonavir-boosted indinavir and efavirenz. *J Infect Dis* 2006; **194**:642–650.
18. Cherry CL, Nolan D, James IR, *et al*. Tissue-specific associations between mitochondrial DNA levels and current treatment status in HIV-infected individuals. *J Acquir Immune Defic Syndr* 2006; **42**:435–440.
19. Jones SP, Qazi N, Morelese J, *et al*. Assessment of adipokine expression and mitochondrial toxicity in HIV patients with lipoatrophy on stavudine- and zidovudine-containing regimens. *J Acquir Immune Defic Syndr* 2005; **40**:565–572.
20. Kim M, Jardel C, Barthelemy C, *et al*. Preserved cytochrome *c* oxidase activity despite mitochondrial DNA depletion in adipose tissue of HIV-infected patients with lipodystrophy. *Antivir Ther* 2005; **10**:L8.
21. Pace CS, Martin AM, Hammond EL, *et al*. Mitochondrial proliferation, DNA depletion and adipocyte differentiation in subcutaneous adipose tissue of HIV-positive HAART recipients. *Antivir Ther* 2003; **8**:323–331.
22. Senior K. Growing old with HIV. *Lancet Infect Dis* 2005; **5**:739.
23. Cherner M, Ellis RJ, Lazzaretto D, *et al*. Effects of HIV-1 infection and aging on neurobehavioral functioning: preliminary findings. *AIDS* 2004; **18 Suppl 1**:S27–34.
24. Hulgan T, Morrow J, D'Aquila RT, *et al*. Oxidant stress is increased during treatment of human immunodeficiency virus infection. *Clin Infect Dis* 2003; **37**:1711–1717.
25. Day BJ, Lewis W. Oxidative stress in NRTI-induced toxicity: evidence from clinical experience and experiments *in vitro* and *in vivo*. *Cardiovasc Toxicol* 2004; **4**:207–216.
26. Ben-Porath I, Weinberg RA. The signals and pathways activating cellular senescence. *Int J Biochem Cell Biol* 2005; **37**:961–976.
27. Dufour E, Larsson NG. Understanding aging: revealing order out of chaos. *Biochim Biophys Acta* 2004; **1658**:122–132.
28. Alexeyev MF, Ledoux SP, Wilson GL. Mitochondrial DNA and aging. *Clin Sci (Lond)* 2004; **107**:355–364.
29. Balaban RS, Nemoto S, Finkel T. Mitochondria, oxidants, and aging. *Cell* 2005; **120**:483–495.
30. Le Bras M, Clement MV, Pervaiz S, Brenner C. Reactive oxygen species and the mitochondrial signaling pathway of cell death. *Histol Histopathol* 2005; **20**:205–219.
31. Dworakowski R, Anilkumar N, Zhang M, Shah AM. Redox signalling involving NADPH oxidase-derived reactive oxygen species. *Biochem Soc Trans* 2006; **34**:960–964.
32. Hayflick L, Moorhead PS. The serial cultivation of human diploid cell strains. *Exp Cell Res* 1961; **25**:585–621.
33. Dimri GP, Lee X, Basile G, *et al*. A biomarker that identifies senescent human cells in culture and in aging skin *in vivo*. *Proc Natl Acad Sci U S A* 1995; **92**:9363–9367.
34. Brookes S, Rowe J, Gutierrez Del Arroyo A, Bond J, Peters G. Contribution of p16(INK4a) to replicative senescence of human fibroblasts. *Exp Cell Res* 2004; **298**:549–559.
35. Chen J, Huang X, Halicka D, *et al*. Contribution of p16INK4a and p21CIP1 pathways to induction of premature senescence of human endothelial cells: permissive role of p53. *Am J Physiol Heart Circ Physiol* 2006; **290**:H1575–1586.
36. Caron M, Auclair M, Vigouroux C, *et al*. The HIV protease inhibitor indinavir impairs sterol regulatory element-binding protein-1 intranuclear localization, inhibits preadipocyte differentiation, and induces insulin resistance. *Diabetes* 2001; **50**:1378–1388.
37. Caron M, Auclair M, Donadille B, *et al*. Human lipodystrophies linked to mutations in A-type lamins and to HIV protease inhibitor therapy are both associated with prelamin A accumulation, oxidative stress and premature cellular senescence. *Cell Death Diff* 2007; **14**:1759–1767.
38. Jan V, Cervera P, Maachi M, *et al*. Altered fat differentiation and adipocytokine expression are inter-related and linked to morphological changes and insulin resistance in HIV-1-infected lipodystrophic patients. *Antivir Ther* 2004; **9**:555–564.
39. Martens UM, Chavez EA, Poon SS, Schmoor C, Lansdorp PM. Accumulation of short telomeres in human fibroblasts prior to replicative senescence. *Exp Cell Res* 2000; **256**:291–299.
40. Arnsten JH, Freeman R, Howard AA, *et al*. HIV infection and bone mineral density in middle-aged women. *Clin Infect Dis* 2006; **42**:1014–1020.
41. Kohli R, Klein RS, Schoenbaum EE, *et al*. Aging and HIV infection. *J Urban Health* 2006; **83**:31–42.
42. Margolick JB, Chopra RK. Relationship between the immune system and frailty: pathogenesis of immune deficiency in HIV infection and aging. *Aging (Milano)* 1992; **4**:255–257.
43. Stoff DM, Khalsa JH, Monjan A, Portegies P. Introduction: HIV/AIDS and Aging. *AIDS* 2004; **18 Suppl 1**:S1–2.
44. Heath KV, Hogg RS, Chan KJ, *et al*. Lipodystrophy-associated morphological, cholesterol and triglyceride abnormalities in a population-based HIV/AIDS treatment database. *AIDS* 2001; **15**:231–239.
45. Miller J, Carr A, Emery S, *et al*. HIV lipodystrophy: prevalence, severity and correlates of risk in Australia. *HIV Med* 2003; **4**:293–301.
46. Appay V, Rowland-Jones SL. Premature ageing of the immune system: the cause of AIDS? *Trends Immunol* 2002; **23**:580–585.
47. Ferrucci L, Cavazzini C, Corsi A, *et al*. Biomarkers of frailty in older persons. *J Endocrinol Invest* 2002; **25**:10–15.
48. Mallon PW, Unemori P, Sedwell R, *et al*. *In vivo*, nucleoside reverse-transcriptase inhibitors alter expression of both mitochondrial and lipid metabolism genes in the absence of depletion of mitochondrial DNA. *J Infect Dis* 2005; **191**:1686–1696.
49. Aure K, Fayet G, Leroy JP, *et al*. Apoptosis in mitochondrial myopathies is linked to mitochondrial proliferation. *Brain* 2006; **129**:1249–1259.
50. Lagathu C, Eustace B, Prott M, *et al*. Some HIV-antiretrovirals increase oxidative stress and alter chemokine, cytokine or adiponectin production in human adipocytes and macrophages. *Antivir Ther* 2007; **12**:489–500.
51. Treitinger A, Spada C, Verdi JC, *et al*. Decreased antioxidant defence in individuals infected by the human immunodeficiency virus. *Eur J Clin Invest* 2000; **30**:454–459.
52. Birkus G, Hitchcock MJ, Cihlar T. Assessment of mitochondrial toxicity in human cells treated with tenofovir: comparison with other nucleoside reverse transcriptase inhibitors. *Antimicrob Agents Chemother* 2002; **46**:716–723.
53. Feng JY, Johnson AA, Johnson KA, Anderson KS. Insights into the molecular mechanism of mitochondrial toxicity by AIDS drugs. *J Biol Chem* 2001; **276**:23832–23837.
54. Smith ED, Kudlow BA, Frock RL, Kennedy BK. A-type nuclear lamins, progerias and other degenerative disorders. *Mech Ageing Dev* 2005; **126**:447–460.

Accepted for publication 30 August 2007